Phase Morphology Development and Melt Rheological Behavior in Nylon 6/Polystyrene Blends

Sobha V. Nair,[1] Zachariah Oommen,[2] Sabu Thomas[1]

[1] *School of Chemical Sciences, Mahatma Gandhi University, Priyadarshini Hills P.O., Kottayam, Kerala, India 686 560*
[2] *Department of Chemistry, C. M. S. College, Kottayam, Kerala, India 686 001*

Received 21 June 2001; accepted 26 February 2002

ABSTRACT: Phase morphology development in immiscible blends of polystyrene (PS)/nylon 6 was investigated. The blends were prepared by melt blending in a twin-screw extruder. The influence of the blend ratio, rotation speed of the rotors, and time of mixing on the phase morphology of the blends was carefully analyzed. The morphology of the samples was examined under a scanning electron microscope (SEM) and the SEM micrographs were quantitatively analyzed for domain-size measurements. From the morphology studies, it is evident that the minor component, whether PS or nylon, forms the dispersed phase, whereas the major component forms the continuous phase. The 50/50 PS/nylon blend exhibits cocontinuous morphology. The continuity of the dispersed phase was estimated quantitatively based on the preferential solvent-extraction technique, which suggested that both phases are almost continuous at a 50/50 blend composition. The effect of the rotor speed on the blend morphology was investigated. It was observed that the most significant breakdown occurred at an increasing rotor speed from 9 to 20 rpm and, thereafter, the domain size remained almost the same even when the rotor speed was increased. The studies on the influence of the mixing time on the blend morphology indicated that the major breakdown of the dispersed phase occurred at the early stages of mixing. The melt rheological behavior of the blend system was studied using a capillary rheometer. The effect of the blend ratio and the shear stress on the melt viscosity of the system was investigated. Melt viscosity decreased with increase in the shear stress, indicating pseudoplastic behavior. With increase of the weight fraction of PS, the melt viscosity of the system decreased. The negative deviation of the measured viscosity from the additivity rule indicated the immiscibility of the blends. The domain size versus the viscosity ratio showed a minimum value when the viscosities of the two phases were matched, in agreement with Wu's prediction. The morphology of the extrudates was analyzed by SEM. From these observations, it was noted that as the shear rate increased the particle size decreased considerably. J Appl Polym Sci 86: 3537–3555, 2002

Key words: morphology; rheology; nylon; polystyrene; scanning electron microscopy

INTRODUCTION

Blending of two or more polymers has proved to be an interesting method to introduce raw materials with tailored properties. There has been an extraordinary growth in the field of polymer-blend production during the last few years compared to homopolymers and copolymers. The reason for this is the possibility for a wider spectrum of applications owing to variable physical properties of the product, depending on its composition.

Nylon 6, an engineering thermoplastic, shows good toughness, strength, abrasion resistance, and chemical resistance. It is widely used for many industrial applications such as in bearings, fishing lines, and ropes and also for the preparation of electrical components. Nylon absorbs water in its molded form, which causes dimensional problems. The water sorption of nylon 6 can be reduced by blending with polystyrene (PS). PS has a high modulus, low water absorption, and good dielectric properties.

It is well established that the properties of a polyblend are determined by the type of morphology and the phase dimensions.[1–4] Therefore, to control the blend properties, the morphology development during processing should be understood. The major factors that influence the morphology and the properties of a polymeric blend include conditions such as temperature, mixing speed, and applied stress. The influence of the mixing time and the blend composition on the structure and rheological and thermal properties of PC/PA6 blends was studied in detail by Gattiglia et al.[5] The effects of the viscosity ratio of the dispersed phase to the matrix on the rheological, morphological, and mechanical properties of blends of PS and two rheologically different LCPs were investigated by Chov et al.[6]

Melt rheological studies of polymers are of great importance in optimizing the processing conditions. These studies are useful in understanding the effect of various parameters on the flow behavior of materials

Correspondence to: S. Thomas (sabuthom@satyam.net.in).

Journal of Applied Polymer Science, Vol. 86, 3537–3555 (2002)

TABLE I
Characteristics of the Materials Used

Material	Source	Density (g/cc)	Molecular weight ($\overline{M}_w$)
PS	Polychem (Mumbai, India)	1.04	3.51×10^5
Nylon 6	DSM (Netherlands)	1.14	2.4×10^4

and in the designing of processing equipment such as injection-molding machines and extruders. Remedies to optimize the processing problems can be suggested by knowing the processing faults and defects.[7] Several studies have been reported on the melt-flow behavior of similar systems. Melt rheological properties of a PS/polyethylene (PE) blend were studied by Van Oene.[8] Utracki and Sammut[9] carried out rheological evolution of a PS/PE blend. The rheological characteristics of some samples of blends of PC with LLDPE were studied by Acierno and Demma.[10] In this laboratory, the melt rheological properties of a series of polymer blends were analyzed.[11–14]

In the present study, nylon/PS blends were prepared by subjecting them to various mixing conditions and the resulting blend morphology was analyzed using a scanning electron microscope (SEM). Both nylon 6 and PS possess different melt viscosities and, therefore, to optimize the processing conditions for these blends, it is necessary to study the effect of shear stress at different temperatures on the viscosity. The objectives of the study included the quantitative analysis of the phase morphology development in PS/nylon blends as a function of the blend composition, mixing time, and speed of the rotors. The phase morphology was studied by SEM, after preferential extraction of the minor component using preferential solvents. Melt rheological properties of the blends were analyzed, giving special emphasis to the effect of the shear rate and the blend ratio on the melt viscosity of the system. Experimental evaluation and theoretical

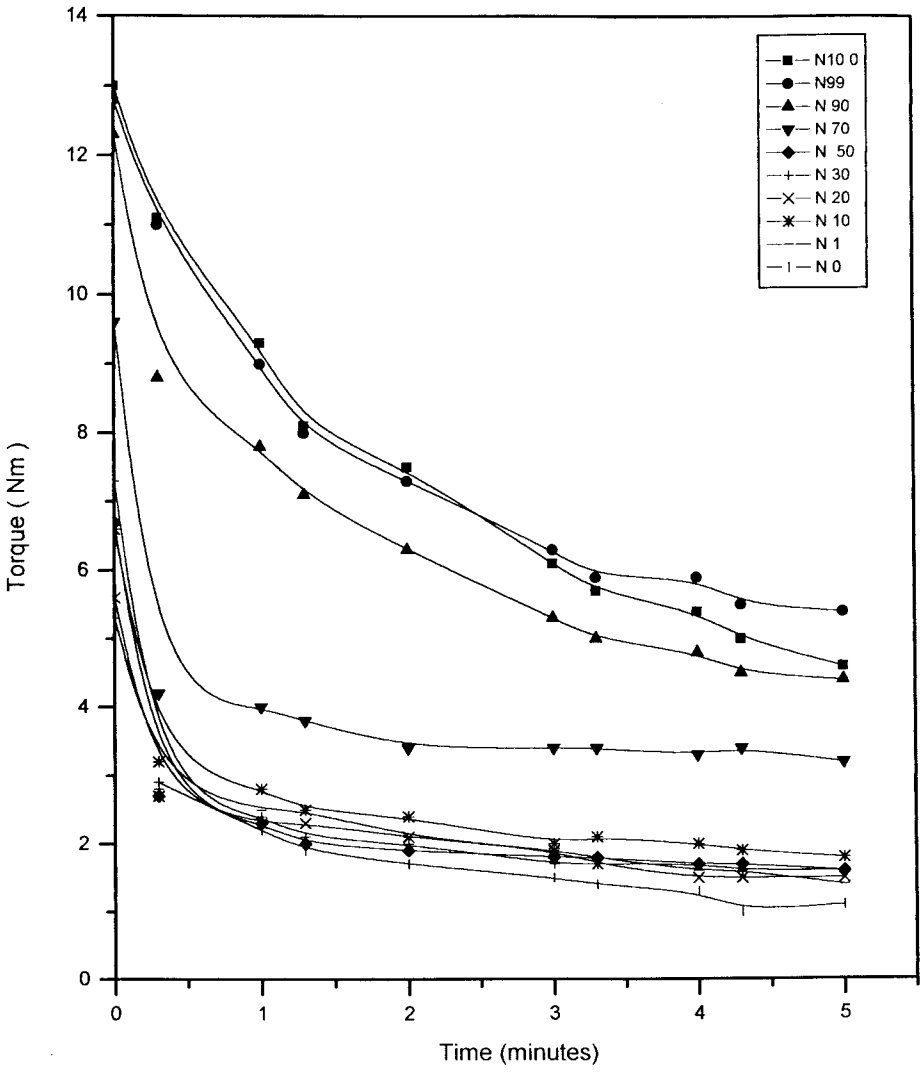

Figure 1 Variation of torque with mixing time.

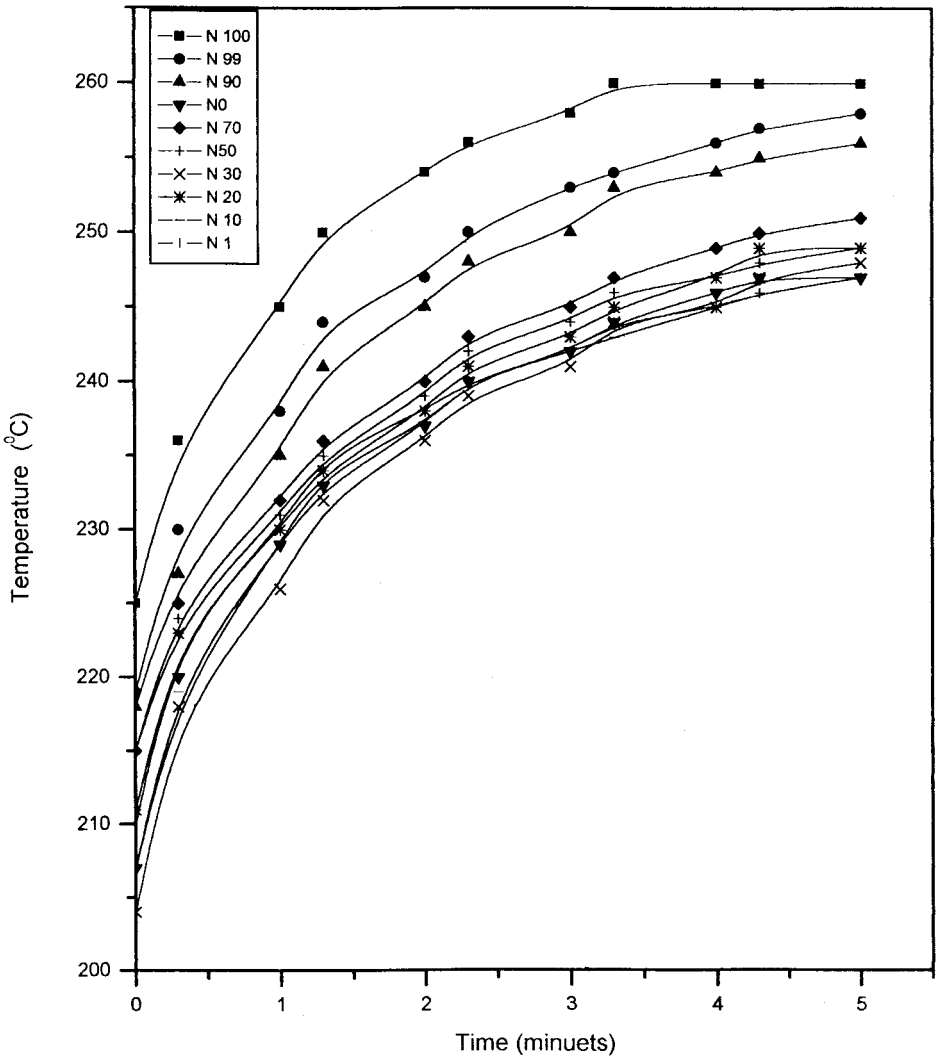

Figure 2 Variation of stock temperature with mixing time.

modeling were used to predict the melt viscosity and phase morphology of the system.

EXPERIMENTAL

Materials

PS was supplied by Poly Chem Ltd. (Bombay, India). Nylon 6 was obtained from DSM (Netherlands). The basic characteristics of PS and nylon 6 are given in Table I.

Preparation of blends

Blends with different compositions [0/100 (N_0), 30/70 (N_{30}), 50/50 (N_{50}), 70/30 (N_{70}), and 100/0 (N_{100})] by weight percentage of nylon/PS were prepared in a corotating twin-screw batch-type miniextruder (DSM) under a nitrogen atmosphere. The subscripts indicate the weight percentage of nylon in the blend. The mixing time, temperature, and rotor speed were 5 min, 250°C, and 100 rpm, respectively. The evolution of the morphology in the blend systems was studied as a function of the blend composition, mixing time, and speed of the rotors. To study the influence of the composition, rotor speed, and mixing time on the blend morphology, experiments were performed as a function of the blend ratio, rotor speed, and time of mixing.

MORPHOLOGY STUDIES

The blend morphology was examined using an SEM (Philips model operating at 10 kV). The samples were fractured under liquid nitrogen and one of the phases was preferentially extracted. For blend samples having a dispersed PS phase, this phase was extracted by using toluene at ambient temperature for a period of 12 h. When nylon formed the dispersed phase, it was extracted by using formic acid at ambient temperature for a period of 12 h. In the case of 50/50 nylon/PS

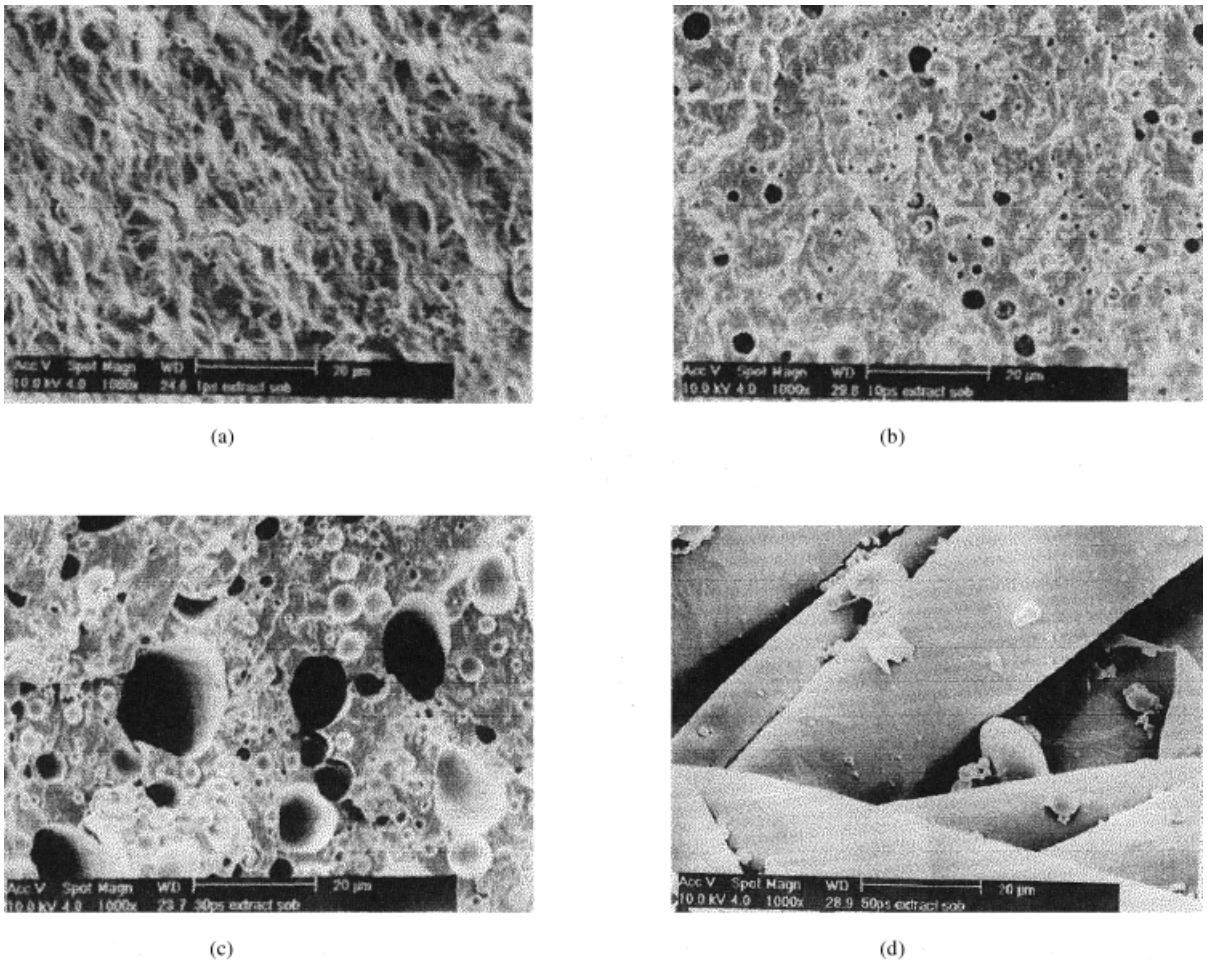

Figure 3 (a–h) SEMs showing the effect of blend composition on phase morphology.

blends having a cocontinuous morphology, the PS phase was extracted. The dried samples were sputter-coated with gold prior to SEM examination. The apparent diameter was measured by scanning the micrographs. Typically, over 400 particles and several fields of view were analyzed. The number-average diameter (D_n), weight-average diameter (D_w), surface area-average diameter (D_s), and volume-average diameter (D_v) were calculated using the following relationships[15]:

Number-average diameter,

$$\bar{D}_n = \frac{\sum N_i D_i}{\sum N_i} \tag{1}$$

Weight-average diameter,

$$\bar{D}_w = \frac{\sum N_i D_i^2}{\sum N_i Di} \tag{2}$$

Surface area-average diameter,

$$\overline{D_s} = \sqrt{\frac{\sum N_i D_i^2}{\sum N_i}} \tag{3}$$

Volume-average diameter,

$$\overline{D_v} = \frac{\sum n_i d_i^4}{\sum n_i d_i^3} \tag{4}$$

where N_i is the number of particles within the diameter range D_i.

Rheological measurements

The shear viscosity of the blends was determined using a capillary rheometer (GOTTFERT Werkstooff-Prufmaschinein GmbH) with an *l/d* ratio of 30 and an angle of entry of 180°. The experiment was done at 230, 240, and 250°C. The shear rates were varied from 5 to 300 s^{-1}. From the apparent shear rate (γ_{ap}) values, the true shear rates (γ_w) were calculated using the following equations:

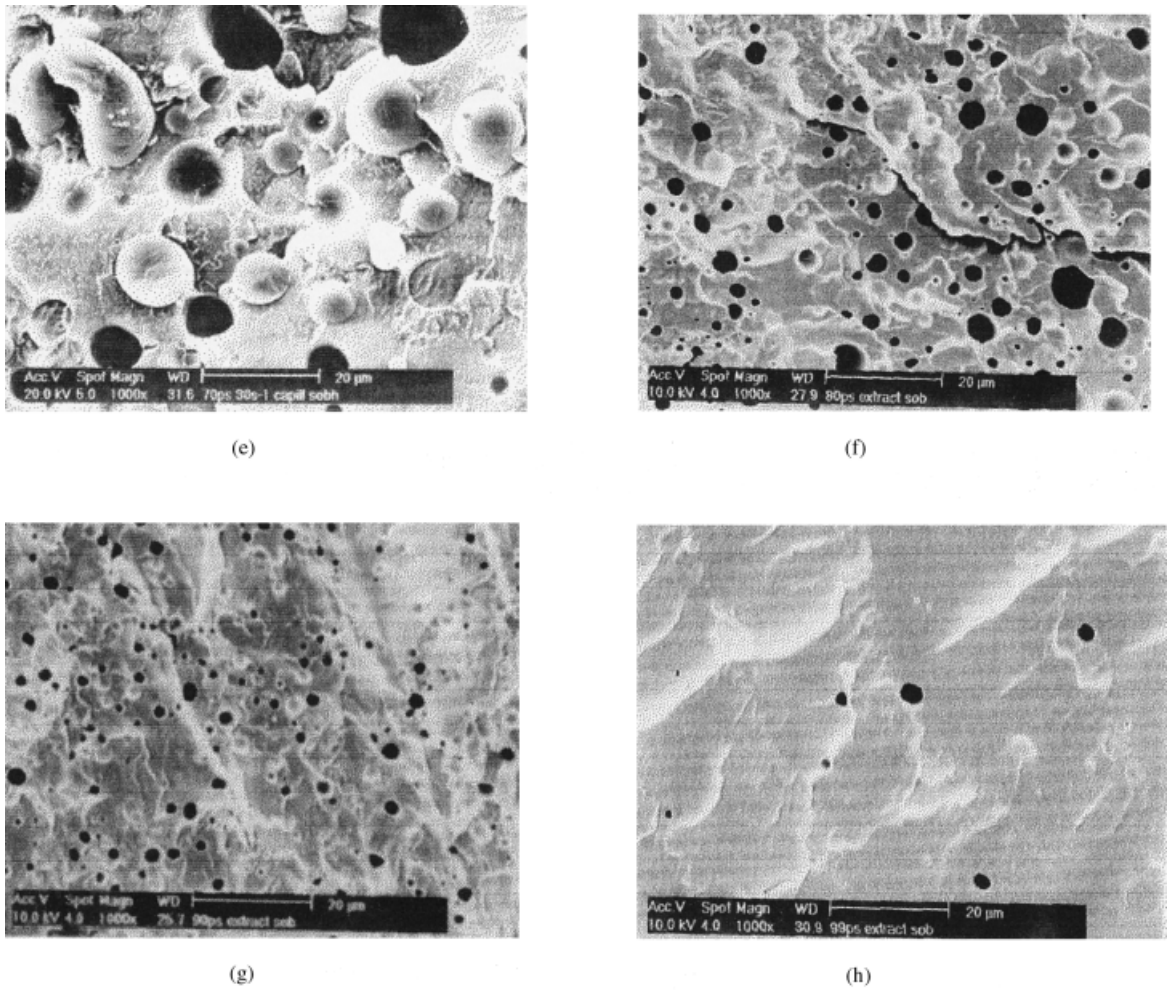

Figure 3 *(Continued from the previous page)*

$$\dot{\gamma}_w = \frac{3n' + 1}{4n'} \dot{\gamma}_{ap} \tag{5}$$

where n' is the flow-behavior index and is defined as

$$n' = \frac{d(\log \tau_w)}{d(\log \dot{\gamma}_{ap})} \tag{6}$$

The flow-behavior index n' is obtained by regression analysis based on the values of τ_w and γ_{ap} obtained from the experimental data. The shear viscosity η was calculated as

$$\eta = \frac{\tau_w}{\dot{\gamma}_w} \tag{7}$$

Extrudate morphology

The morphology of the fractured samples was examined under an SEM. However, in certain cases, to have contrast, the minor phase from the extrudate was extracted by immersion in the respective solvents suitable for the preferential extraction of one of the phases. The nylon 6 phase was extracted using formic acid, and PS, by toluene. The samples were then dried in an air oven and the extracted surface was examined under an SEM.

RESULTS AND DISCUSSION

Mixing characteristics

The final morphology of the blends has a controlling influence on the properties of the blend. The mixing characteristics of the PS/nylon blends presented in Figures 1 and 2 represent the variation of the mixing torque and the stock temperature, developed with the time of mixing. It is evident from Figure 1 that, in all cases, the torque decreases with the mixing time and levels off at 4–5 min of mixing. The torque first increases quickly as the cold material is fed into the mixer. As the material is heated by shear and thermal means, it softens and the torque falls. The torque then levels off to a nearly constant value for the remaining of the mixing time. The leveling-off in the torque can be

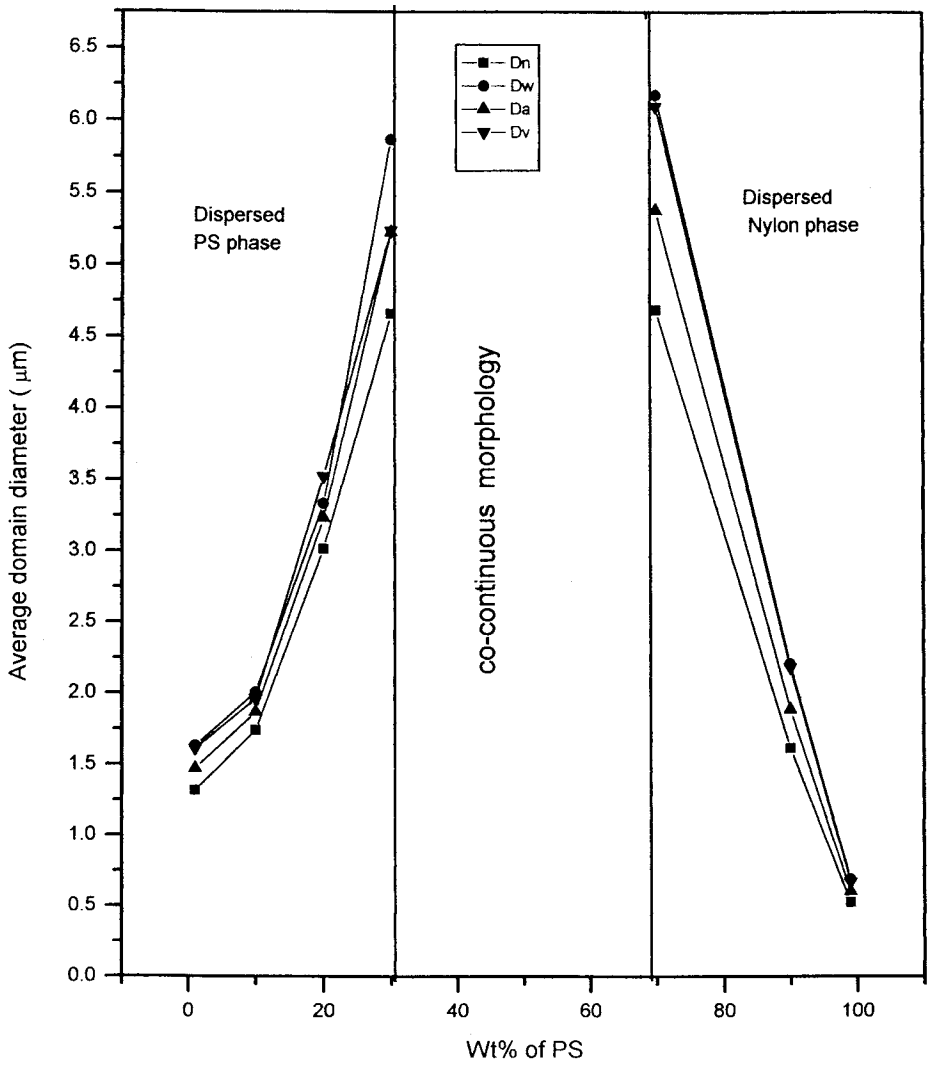

Figure 4 Effect of blend composition on particle size.

attributed to a good level of mixing of the components. The initial and final torque values of the blends increase with the nylon content, as nylon 6 has a high melt viscosity compared to PS. The stock temperature of the blends is initially low as a result of feeding the material at room temperature. The stock temperature increases with the mixing time and tends to level off (Fig. 2).

TABLE II
Interfacial Area per Unit Volume of the Blends

Wt % of PS	Volume fraction of the dispersed phase (ϕ_A)	Interfacial area per unit volume (μm^{-1})
1	0.0109	0.0625
10	0.1806	0.4022
30	0.3196	0.4091
80	0.1857	0.3690
90	0.0920	0.3110
99	0.0091	0.0207

Effect of composition on morphology

Morphology development is the evolution of the blend morphology from pellet-sized or powder-sized

TABLE III
Percentage of Continuity by Solvent Dissolution

Dispersed phase concentration	Continuity of phases
PS dispersed	Continuity of PS phase (%)
1	2
10	11
30	22
50	88
Nylon dispersed	Continuity of nylon phase (%)
1	0.03
10	1
20	5
30	29
50	85

TABLE IV
Modeling of Phase Inversion

η Ratio	Jordhamo		Chen and Su		Chen and Su (mod)	
	ϕ_{PS}	ϕ_N	ϕ_{PS}	ϕ_N	ϕ_{PS}	ϕ_N
4.460	0.1832	0.8168	0.3473	0.6527	0.3897	0.6103
5.2315	0.1604	0.8396	0.3365	0.6635	0.3810	0.6190
5.3992	0.1563	0.8437	0.3762	0.6238	0.3762	0.6238
5.5638	0.1523	0.8396	0.3324	0.6676	0.3740	0.6260
6.0209	0.1423	0.8577	0.3272	0.6728	0.3685	0.6315
7.6457	0.1156	0.8843	0.3022	0.6978	0.3520	0.6480
8.6010	0.1402	0.8958	0.2951	0.7049	0.3897	0.6560

Experimental observation of phase inversion is found to occur at $\phi_{PS} = 0.5229$ and $\phi_N = 0.4771$.

particles to the submicrometer droplets which exist in the final blend. When two immiscible polymers are blended during melt extrusion, one phase is mechanically dispersed into the other one. The size and the shape of the dispersed phase depend on several processing parameters, including the rheology, interfacial properties, and the composition of the blend. By changing the dispersed phase concentration, we follow the coalescence process equilibrium during mixing. As reported by Danesi and Porter,[16] for blends with the same processing history, the melt viscosity ratio and composition determine the morphology. The least viscous component was observed to form the continuous phase over a wide range of composition.

The phase morphology of the blends over a composition range from 1/99, 10/90, 30/70, 50/50,70/30, 80/20, 90/10 to 99/1 PS/nylon 6 blends can be understood from the SEM photomicrographs given in Fig-

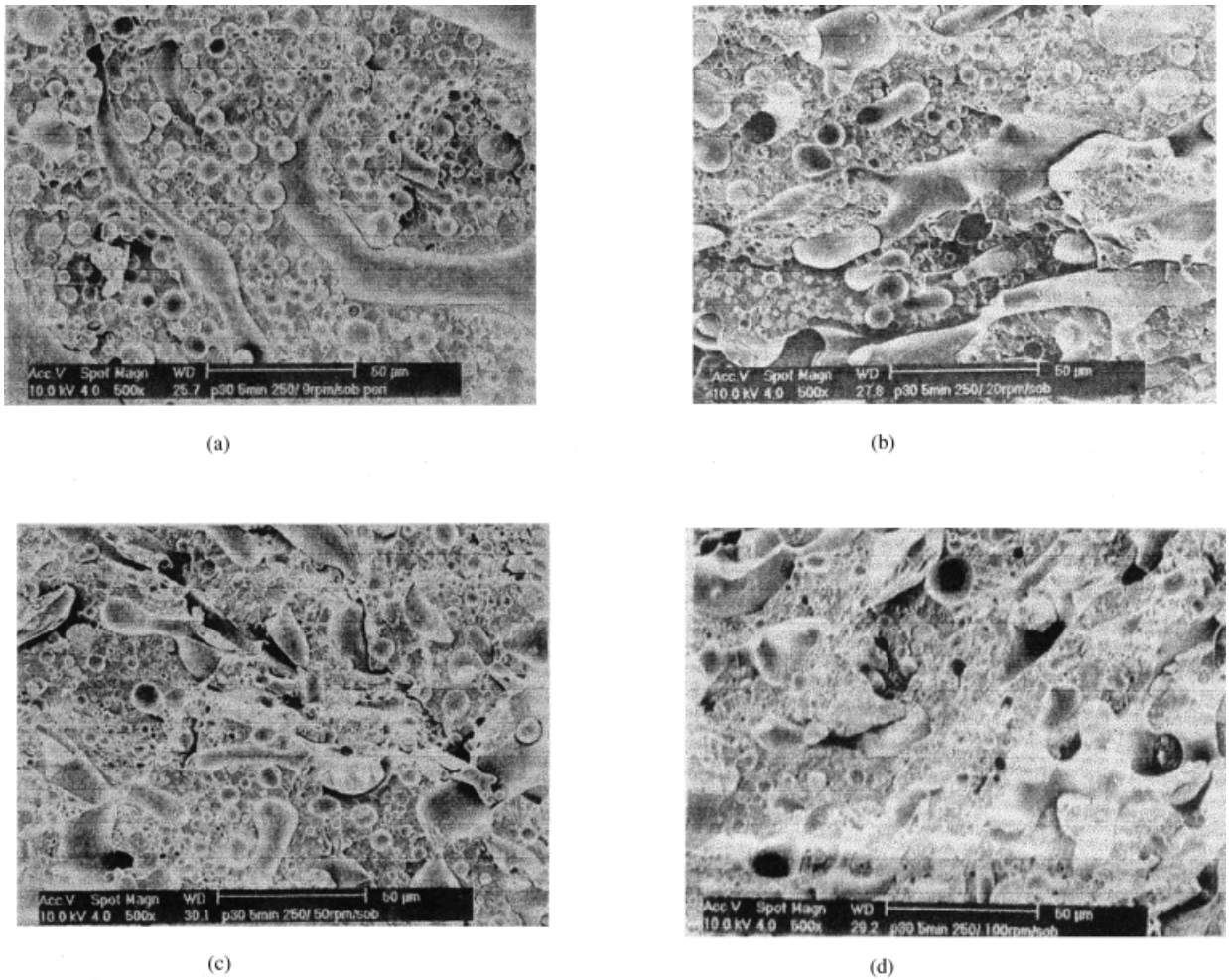

Figure 5 (a–d) SEMs showing the effect of rotor speed on phase morphology.

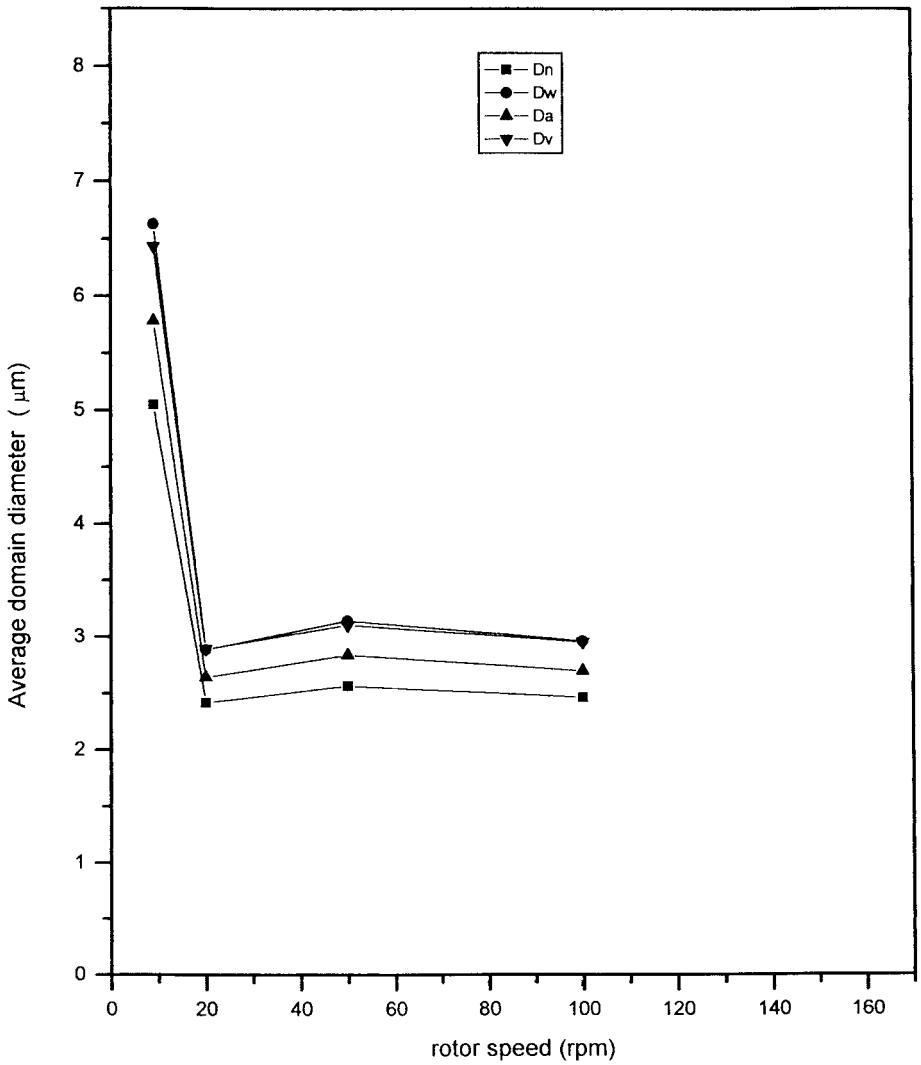

Figure 6 Effect of rotor speed on particle size.

ure 3(a–h). The minor phase in each composition was extracted with proper solvents. PS was extracted using toluene, and nylon, using formic acid. It is evident from the SEM photomicrographs that the component with the low weight percentage is the dispersed phase and the other one forms the continuous phase. It can be seen that, as the concentration of the dispersed phase increases, the domain size increases. At a 50/50 PS /nylon concentration, a cocontinuous morphology is exhibited by the system, which is again confirmed by the extraction experiment. Fibrillar structures were observed in the SEM of 50/50 composition from which the PS phase is extracted, which suggests that nylon is fibrilized at a 50/50 composition. The fiber formation is considered to be a result of the stretching and coalescence of individual particles.[17] In the case of blends, the component with more crystallinity and melt viscosity will have a tendency to fibrillate under shear. Thus, in the case of nylon/ PS blends, which exhibit cocontinuous morphology, the nylon phase, having higher melt viscosity as well as crystallinity, exhibits fibrillar morphology.

Figure 4 depicts the number-average, weight-average, surface-average, and volume-average particle diameters as a function of the PS concentration. In two-phase dispersed polymer systems, it is primarily the rheological factors which control the morphology of the blend in a given flow field. Straita[18] and Heikens et al.[19] reported that the composition ratio and the viscosity ratio of individual components determine the morphology of the melt-mixed polymer blend. When the minor component has a higher viscosity than that of the major component, the minor component is coarsely dispersed. On the other hand, the minor component is finely dispersed when it has a lower viscosity than that of the major component. Several authors have reported on the phenomenon of coalescence in solvent-cast or melt blends. The phenomenon of coalescence at a higher concentration of one of the components was reported by Dao,[20] Heikens and Barensten,[21] and

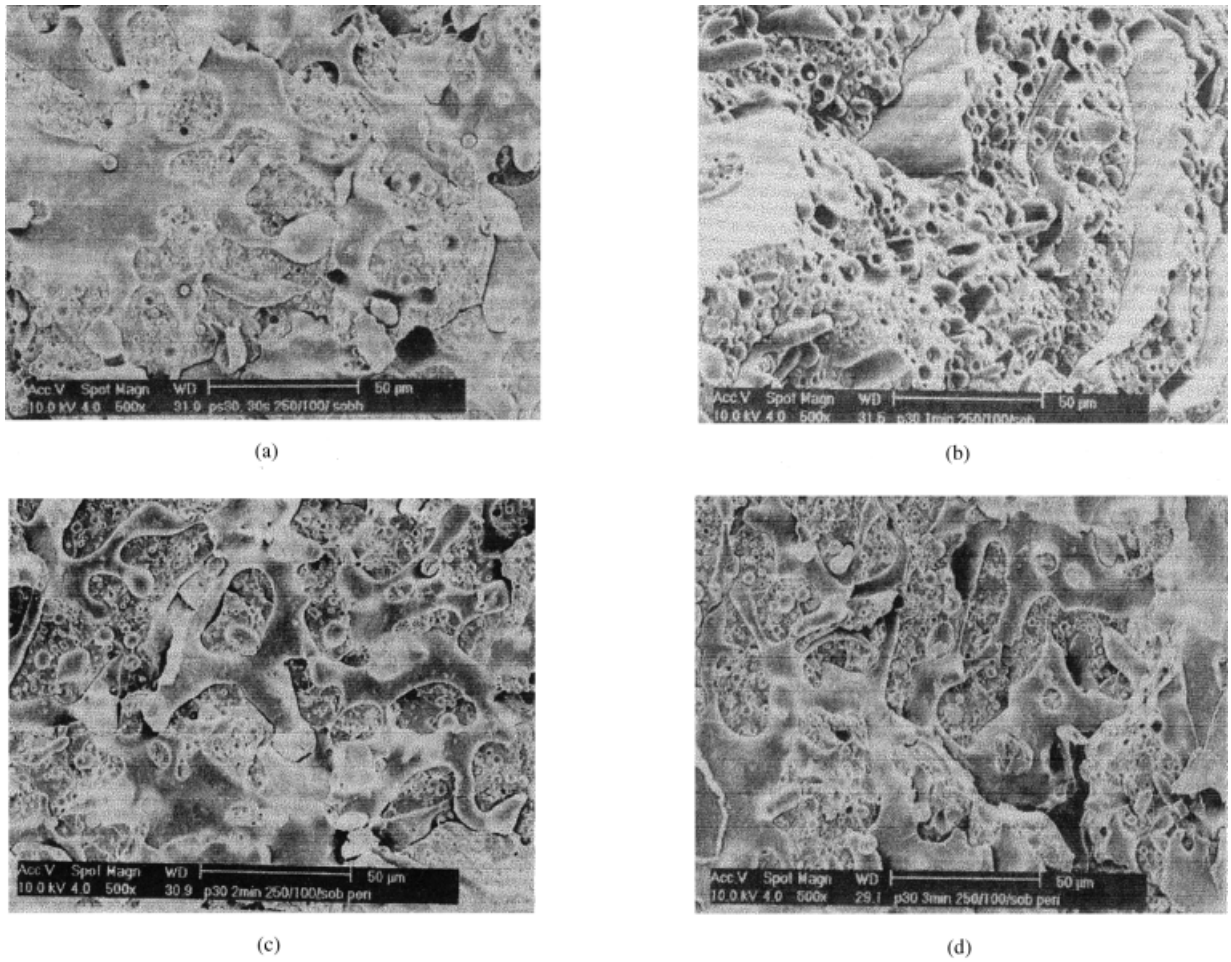

Figure 7 (a–h) SEMs showing the influence of mixing time on phase morphology.

Thomas and Groeninckx.[22] At a low enough concentration of the dispersed phase, only breakup should occur and there is a limiting drop size. On the other hand, when PS forms the dispersed phase, the rate of coalescence is lower due to the high viscosity of the nylon phase, which forms the matrix phase.

Let us consider a binary blend that contains a volume fraction ϕ_A of polymer A as spherical domains of radius R in a B matrix. The interfacial area per unit volume of the original blend is equal to $3\phi_A/R$ (ref. 23). The interfacial area per unit volume of the blend is calculated and the results are summarized in Table II. It is evident from Table II that blends with PS as the dispersed phase have a large interfacial area. This indicates that the domain size of the dispersed PS phase is lower than when nylon is the dispersed phase. When nylon with a high melt viscosity is dispersed in a low viscous PS phase, there is a great chance for coalescence of the dispersed nylon particles because of the high diffusional mobility of nylon domains in the low-viscosity PS phase. This leads to an increase in the domain size of the dispersed nylon phase and, consequently, a low interfacial area. With increase in the nylon concentration, the coalescence rate increases, resulting in an increased domain diameter and, therefore, the interfacial area is further reduced.

Continuity and phase inversion

It is evident from the SEM that 50/50 PS/nylon blends exhibit a cocontinuous morphology. The development of continuity as described by the percolation theory can be summarized as follows: Initially, at low concentrations, there is a dispersion of particles in the matrix. As the concentration of the minor phase increases, particles become close enough to behave as if they were connected. Further addition of minor-phase material extends the continuity network until the minor phase is continuous throughout the sample.

In the present study, the continuity of the dispersed phase was calculated by the solvent-dissolution method.[24] PS, when it forms the minor phase, was extracted using toluene, and nylon 6, using formic acid. When the samples with a concentration of PS above 50 wt % were kept in toluene, a jelly mass was obtained, suggesting that PS is continuous in these

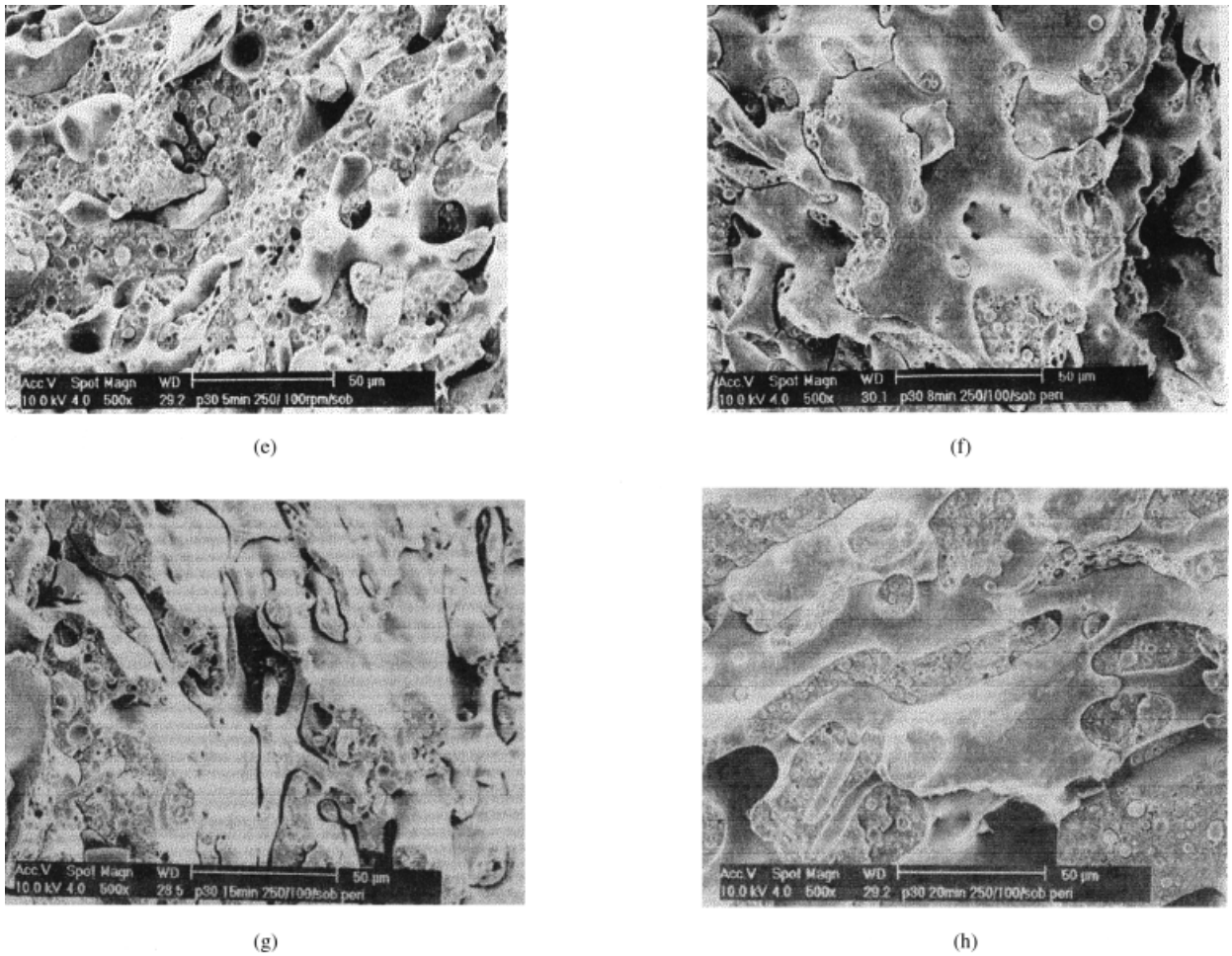

Figure 7 *(Continued from the previous page)*

blend compositions. Continuity of the component is defined as the ratio of the difference of the weight of the component present initially and the calculated weight of the residual component after extraction to the weight of the component present initially:

$$\text{Continuity} = \frac{\text{initial weight of the component} - \text{weight after extraction}}{\text{initial weight of the component}} \quad (8)$$

The results are summarized in Table III. From the values, it is evident that the continuity of both phases approaches 90% in the 50/50 blend composition, which is in agreement with SEM photographs that show a cocontinuous morphology for 50/50 PS/ nylon blends. For the other blend compositions (N_1, N_{10}, N_{30}, N_{70}, N_{90}, and N_{99}), the continuity is less than even 30%, suggesting a dispersed-phase morphology.

Various models have been applied for the prediction of a continuity point. Jordhamo et al.[25] developed an empirical model based on the melt viscosity ratio, η_d/η_m, and the volume fractions, ϕ, of each phase for predicting the phase inversion in immiscible polymer blends. According to this model, phase inversion should occur when

$$\frac{\eta_1}{\eta_2}\frac{\phi_2}{\phi_1} = 1 \quad (9)$$

Chen and Su[26] proposed the following equation, taking into account the fact that the Jordhamo model overestimates the volume fraction of the high viscosity phase:

$$\frac{\phi_{hv}}{\phi_{lv}} = 1.2\left(\frac{\eta_{hv}}{\eta_{lv}}\right)^{0.3} \quad (10)$$

The region of phase inversion can also be modeled using a modified Chen and Su model by avoiding 1.2 from the above equation[27]:

$$\frac{\phi_{hv}}{\phi_{lv}} = \left(\frac{\eta_{hv}}{\eta_{lv}}\right)^{0.3} \quad (11)$$

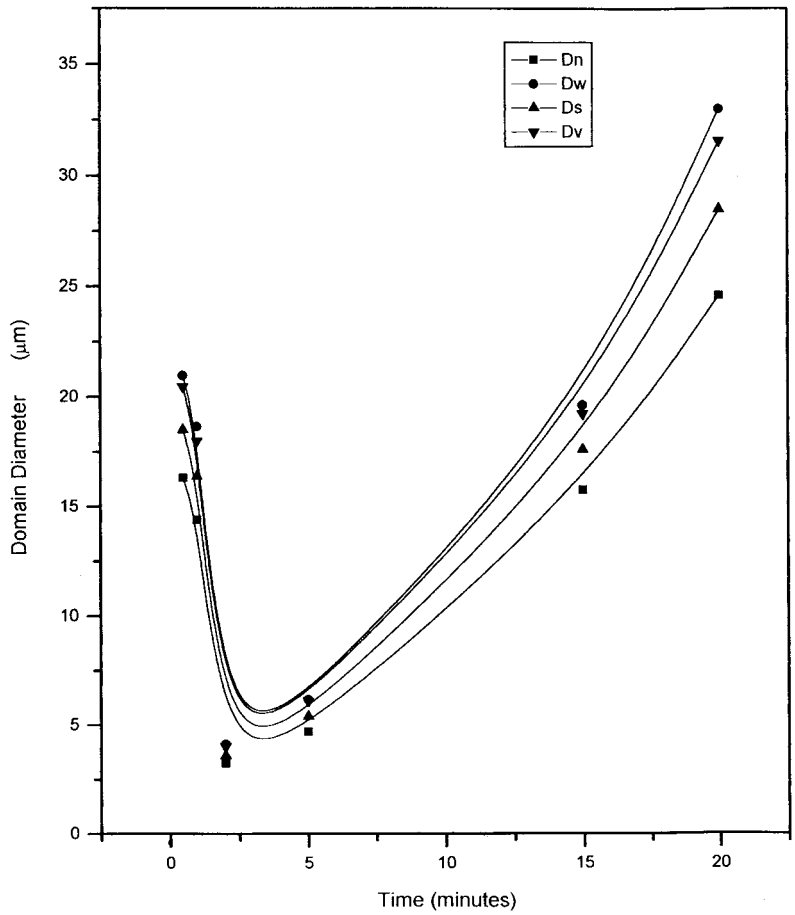

Figure 8 Effect of mixing time on particle size.

The volume fractions of PS and nylon at their phase-inversion points as predicted by these models are given in Table IV. The phase-inversion point in the PS/nylon system does not agree with any of the three models. The variation of the phase-inversion points obtained from SEM and the solvent-dissolution technique suggests that these models require some modification. Of the models applied, a modified Chen and Su equation predicts the phase-inversion point closer to the experimental observation. In all these models, the only factor that was taken into account was the viscosity ratio of the components at different shear rates. Hence, it appears that the viscosity ratio alone is not sufficient to predict the phase-inversion point in all circumstances. Apparently, other parameters, including the interfacial tension, absolute values of the viscosity rather than their ratio, phase dimensions, and mixing conditions have an effect on the formation of cocontinuous structures.

Influence of rotor speed on dispersed-phase size

The dependence of the dispersed-phase size on the rotation speed of the rotors was studied. SEM photomicrographs for 70/30 nylon/PS blends mixed at 9, 20, 50, and 100 rpm are shown in Figure 5(a–d), respectively. The melt mixing was done at 250°C for 5 min. The domain diameter was plotted as a function of the rotor speed in Figure 6. It is evident from the plot that the most significant breakdown takes place by increasing the rotor speed from 9 to 20 rpm. A further increase in the rotor speed does not have any influence on the morphology. Many authors have studied the dependence of phase dimension on the shear stress and shear rate. Mine et al.[28] reported large differences in the morphology with changing shear stress: Coalescence during mixing will be governed by interfacial mobility. However, Elmendrop and vander Vegt[29] found, experimentally, that polymers had a high coalescence probability during mixing and concluded that polymers had fully mobile interfaces. Roland and Bohm[30] found that an increasing shear rate, which intuitively is expected to decrease coalescence, actually increased coalescence.

In the present study, by increasing the rotor speed from 20 to 100 rpm, the drop size is not affected and the most significant breakdown took place within a range of 9–20 rpm. If the rpm of the rotor is considered to be proportional to the shear rate, then it is seen

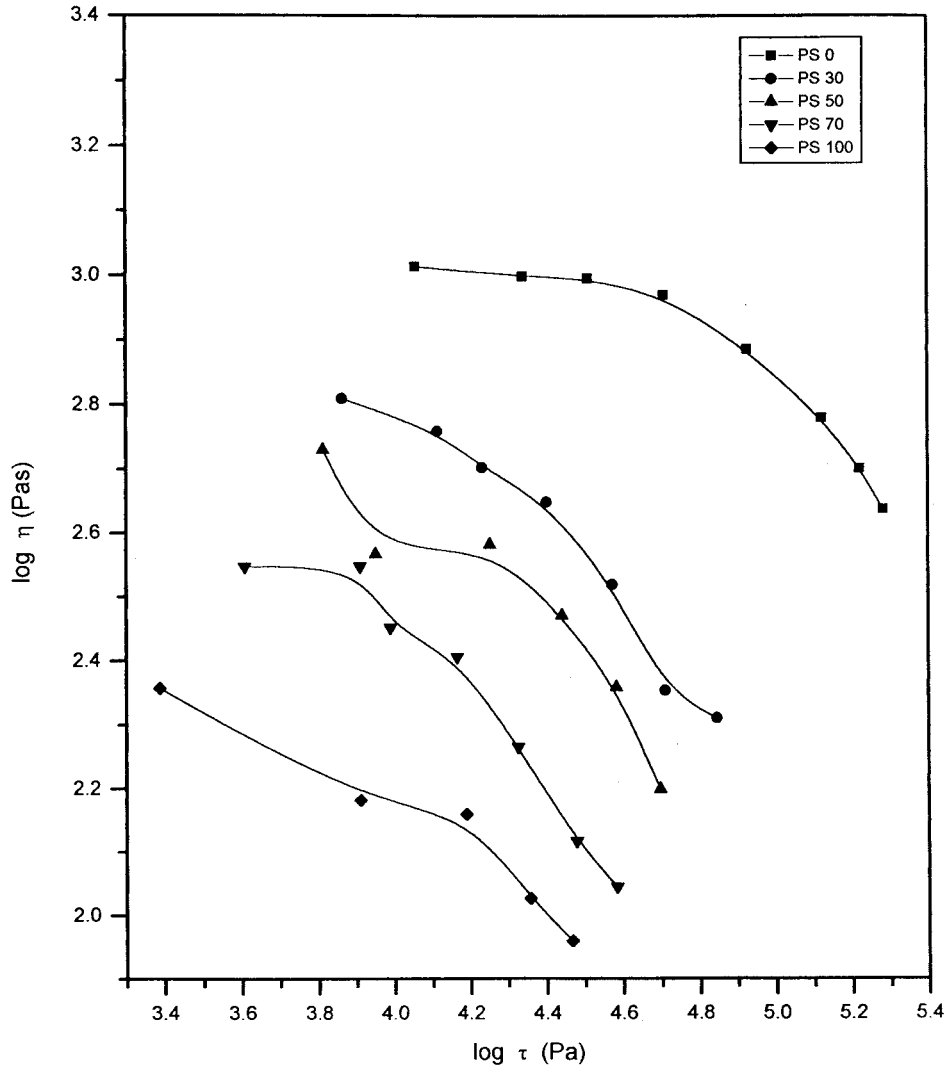

Figure 9 Effect of shear stress on melt viscosity.

from the figure that the domain size is hardly affected when there is about a twofold increase in rpm.

Studies of Taylor[31,32] analyzed the breakup of a single Newtonian drop in a simple shear field. Taylor modeled the drop size using the viscosity ratio $\eta_r = \eta_d / \eta_m$ and the capillary number

$$Ca = \frac{\dot{\gamma}\eta_m D}{2\Gamma} \tag{12}$$

where D is the diameter of the droplet; γ, the shear rate; η_m, the matrix viscosity; and Γ, the interfacial tension. Studies of Favis[33] and Sundararaj et al.[34] suggested that, above a critical shear stress, the blends are not highly sensitive to either the shear stress or shear rate, which is unexpected based on Taylor's theories. In the present study also, it is evident that, beyond a certain shear rate, there is no further reduction in the domain size. This variation can be attributed to that the shear stress and the shear rates are not continuous at the interface. The variation from Taylor's prediction can be accounted for by polymer elasticity. When the shear rate is increased, the matrix viscosity decreases and the drop elasticity increases, so that the drop resists deformation to a greater extent. Hence, there is an optimum shear rate where the finest dispersion is obtained.

Influence of mixing time on morphology

Figure 7(a–h) shows the morphology of the 30/70 PS/nylon blends mixed for 0.5, 1, 2, 3, 5, 9, 15, and 20 min, respectively. The influence of the mixing time on the domain diameter is represented in Figure 8. The mixing was done at a rotor speed of 100 rpm at a temperature of 230°C. It can be seen from the SEM photomicrographs that the most significant breakdown takes place within the first 3 min of mixing, where there is melting and consequent liquefaction. The main mechanism governing the morphology development is believed to be the result of both droplet

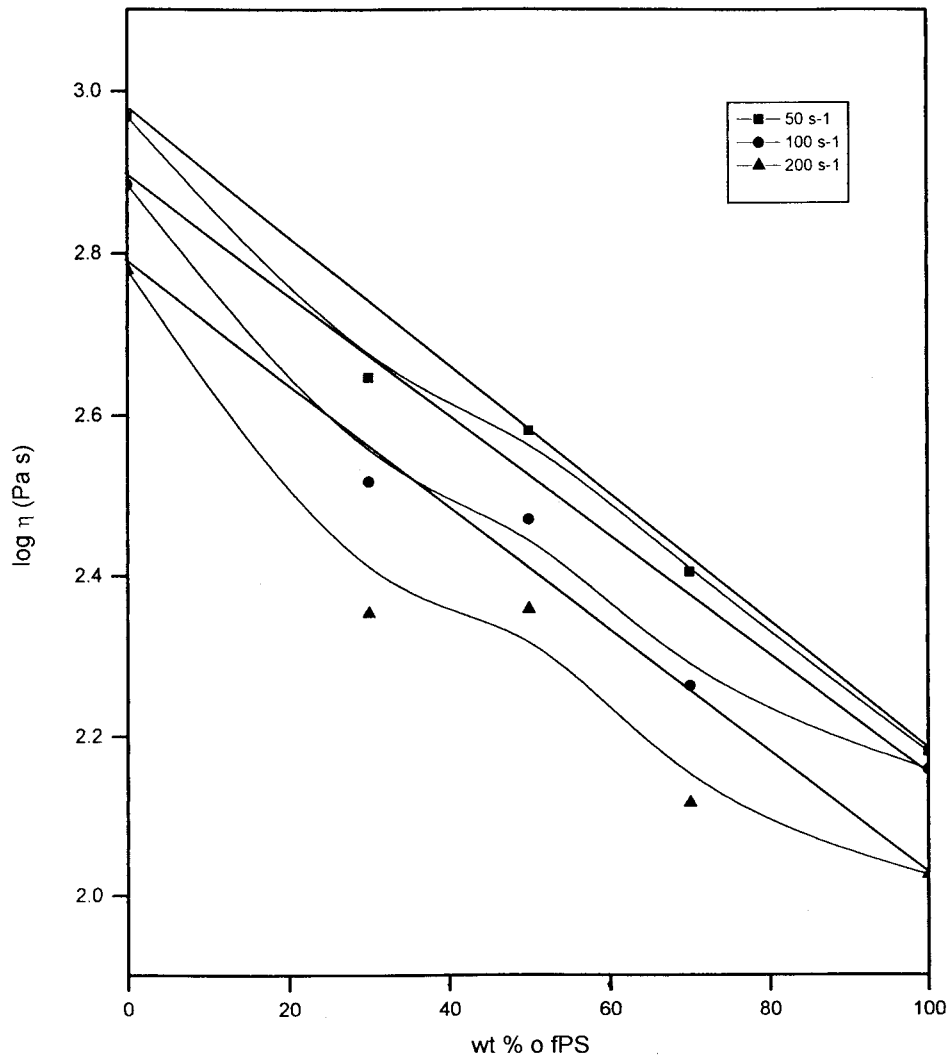

Figure 10 Effect of blend composition on melt viscosity.

breakup and coalescence. Several studies are reported on the effect of mixing time on the blend morphology. These results, including our present study, are in agreement with Taylor's equation, which suggests that there is a critical value of the Weber number below which no particle deformation takes place and, as a result, a critical particle size. For viscoelastic systems like polymer blends, as the individual components exhibit large normal stresses in flow, the extension of Taylor's analysis to such systems has some limitations. Wu[35] gave a correlation relating the capillary number to the viscosity ratio in extruded polymer blends. According to this,

$$D = \frac{4\tau\eta_\gamma^{\pm 0.84}}{\dot{\gamma}\eta_m} \tag{13}$$

where the + sign in the exponent applies to $\eta_r > 1$ and the − sign applies to $\eta_r < 1$.

Wu's correlation suggests a minimum particle size when the viscosities of the two phases are closely matched. The increase in the phase dimension at longer mixing times is associated with shear-induced coalescence. It was reported that the contact time required for drop coalescence increases when the drop diameter increases, the matrix viscosity increases, and the density difference between the drop and the matrix phase increases.[36]

The studies of Schreiber and Olguin[37] reported that bulk particle-size reduction takes place very early in the mixing process. The dependence of the phase size versus the energy leveled off very rapidly. Thomas and Groeninckx[22] reported that the major breakdown of particles occurs at the very beginning of the mixing process for EPM/nylon 6 blends. In the present study, the major breakdown occurs during the early stages of mixing. This is in agreement with Taylor's theory, which suggests that there is a

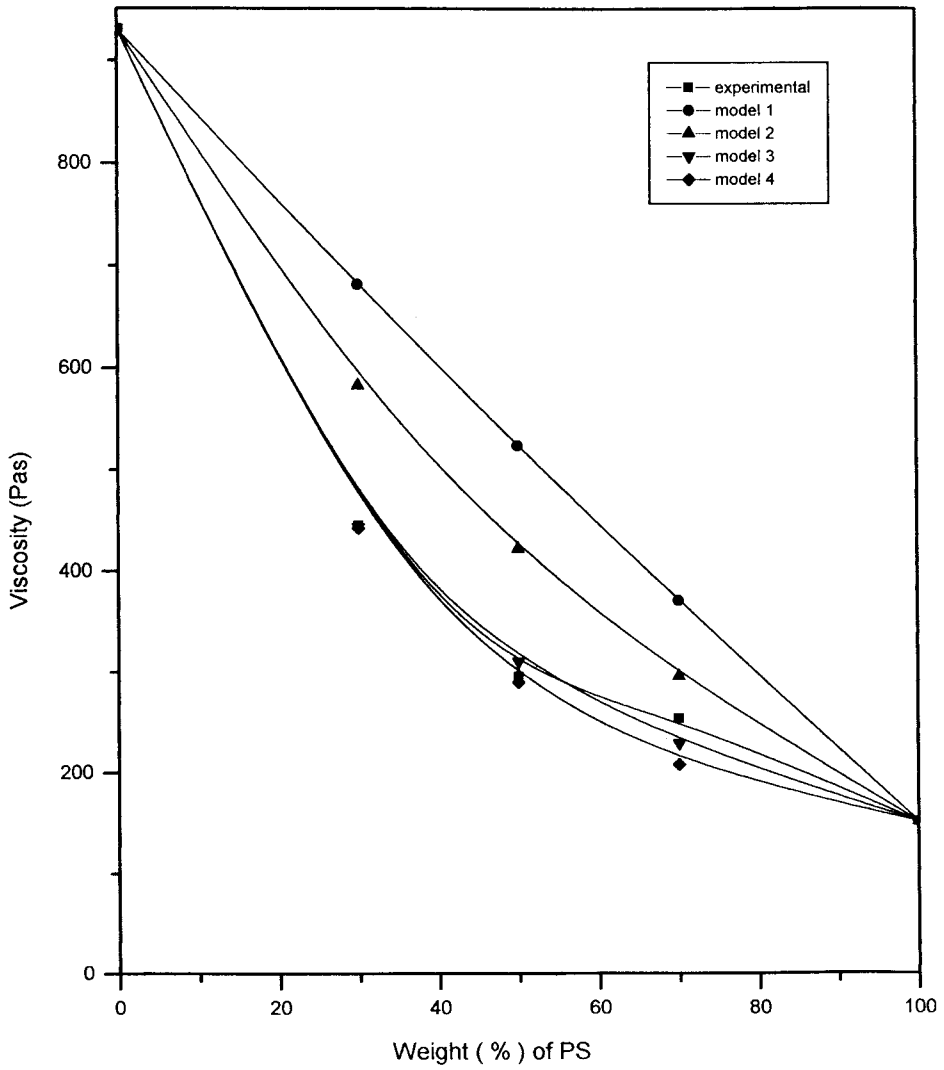

Figure 11 Theoretical modeling of melt viscosity.

critical value of the Weber number below which no particle deformation takes place and, as a result, a critical particle size. This study further indicates that the initial melting and liquefaction period is highly important since the final morphology is generated during this period.

Melt rheology

Effect of shear–stress and blend ratio on viscosity

The effects of the shear stress and blend composition on the melt viscosity of the nylon/PS blend system were analyzed. The results are presented in Figures 9 and 10. It is evident from the plots that the viscosity of the system decreases with increase in the shear stress, indicating the pseudoplastic nature of the blend systems. At zero shear, the molecules are randomly oriented and highly entangled and, hence, exhibit high viscosity. Under the application of a shearing force, the polymer chains orient and get disentangled, resulting in reduced viscosity at high shear stress. The reduction in viscosity of the blends at a higher shear rate is also due to the decrease in the particle size. At a given shear stress, the melt viscosity is lowest for pure PS and the highest for pure nylon. When nylon is added to the PS, the viscosity increases with the nylon content at all shear stresses. In polymer blends, the viscosity depends on the interfacial adhesion in addition to the characteristics of the component polymers. This is because, in polymer blends, there is interlayer-slip along with the orientation and disentaglement upon the application of shear stress. When shear stress is applied to a blend, it undergoes an elongational flow. If the interface is strong, the deformation of the dispersed phase is effectively transferred to the continuous phase. However, in the case of a weak interface, interlayer slip occurs, and as a result, the viscosity of the system decreases. From Figure 10, it can be

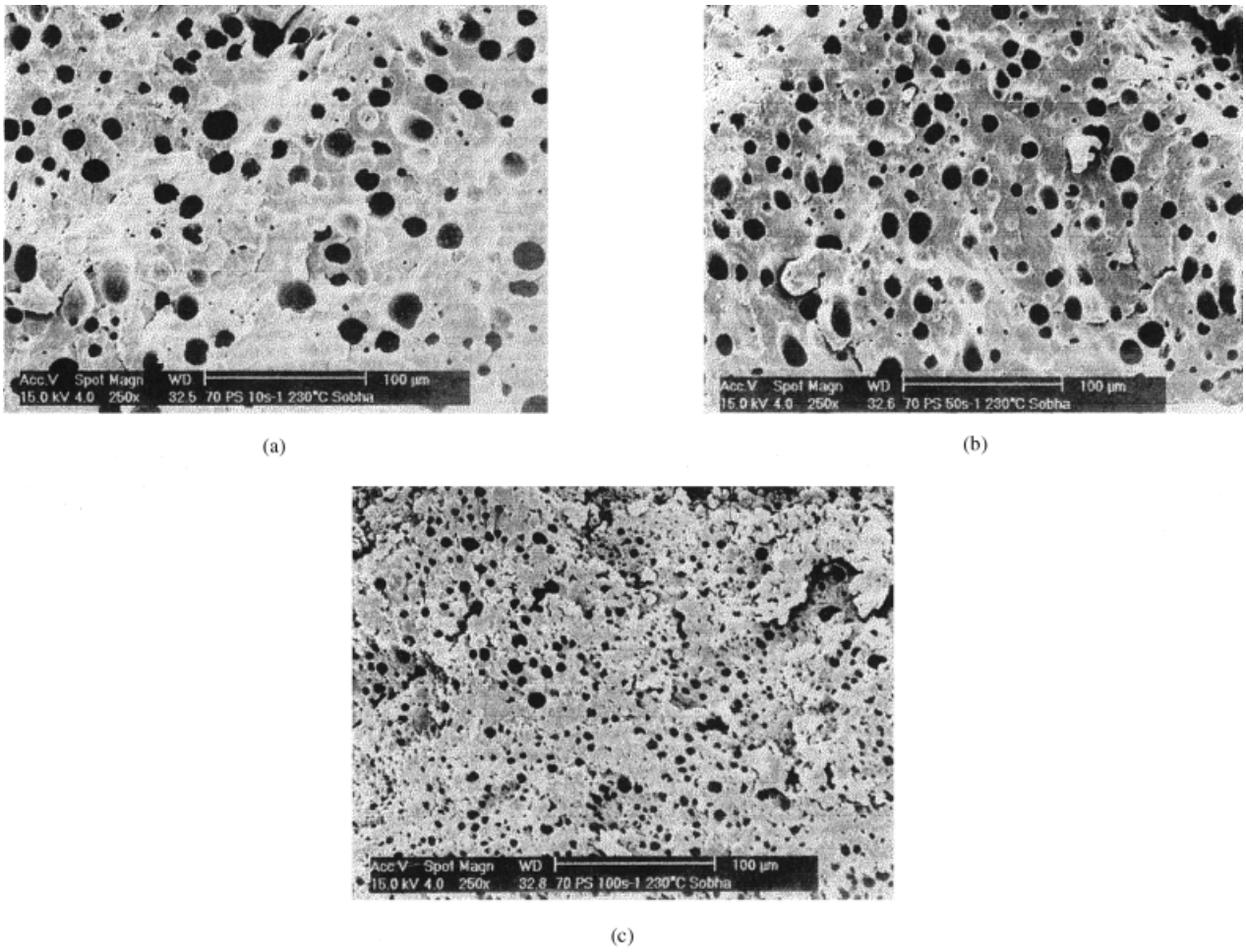

Figure 12 (a–c) SEMs showing the effect of shear rate on particle size.

seen that variation of the melt viscosity versus the blend composition is nonlinear, showing negative deviation with respect to the linear extrapolation between the PS and nylon 6 extremes.

Comparison with theoretical predictions

The viscosity of the blends was correlated with various theoretical models. Utracki and Sammut[38] showed that a positive or negative deviation of the measured viscosity from that calculated from the log additivity rule is an indication of strong or weak interactions between the phases of the blend:

$$\ln(\eta_{ap})\text{blend} = \sum w_i \ln(\eta\text{app})_I \qquad (14)$$

where w_i is the weight fraction of the i^{th} component of the blend. They indicated that the negative deviation shown by the immiscible blends is associated with the heterogeneous nature of the components, whereas a positive deviation indicates the miscibility of the blends resulting from the high solubility and homogeneous nature of the components. According to the rule of additivity,

$$\eta_{mix} = \eta_1\phi_1 + \eta_2\phi_2 \qquad \text{Model 1} \qquad (15)$$

where η_1 and η_2 are the viscosities of the components and ϕ_1 and ϕ_2 are their volume fractions.

Hashin's upper- and lower-limit models predict the viscosities by the following equations:

$$\eta_{mix} = \eta_2 + \frac{\phi_1}{\dfrac{1}{(\eta_1 - \eta_2)} + \dfrac{\phi_2}{2\eta_2}} \qquad \text{Model 2} \qquad (16)$$

$$\eta_{mix} = \eta_1 + \frac{\phi_2}{\dfrac{1}{(\eta_2 - \eta)_1} + \dfrac{\phi_1}{2\eta_1}} \qquad \text{Model 3} \qquad (17)$$

η_1, η_2, ϕ_1, and ϕ_2 are the same as before.

Sood et al.[39] developed an altered free-volume model to calculate the viscosity. According to this model,

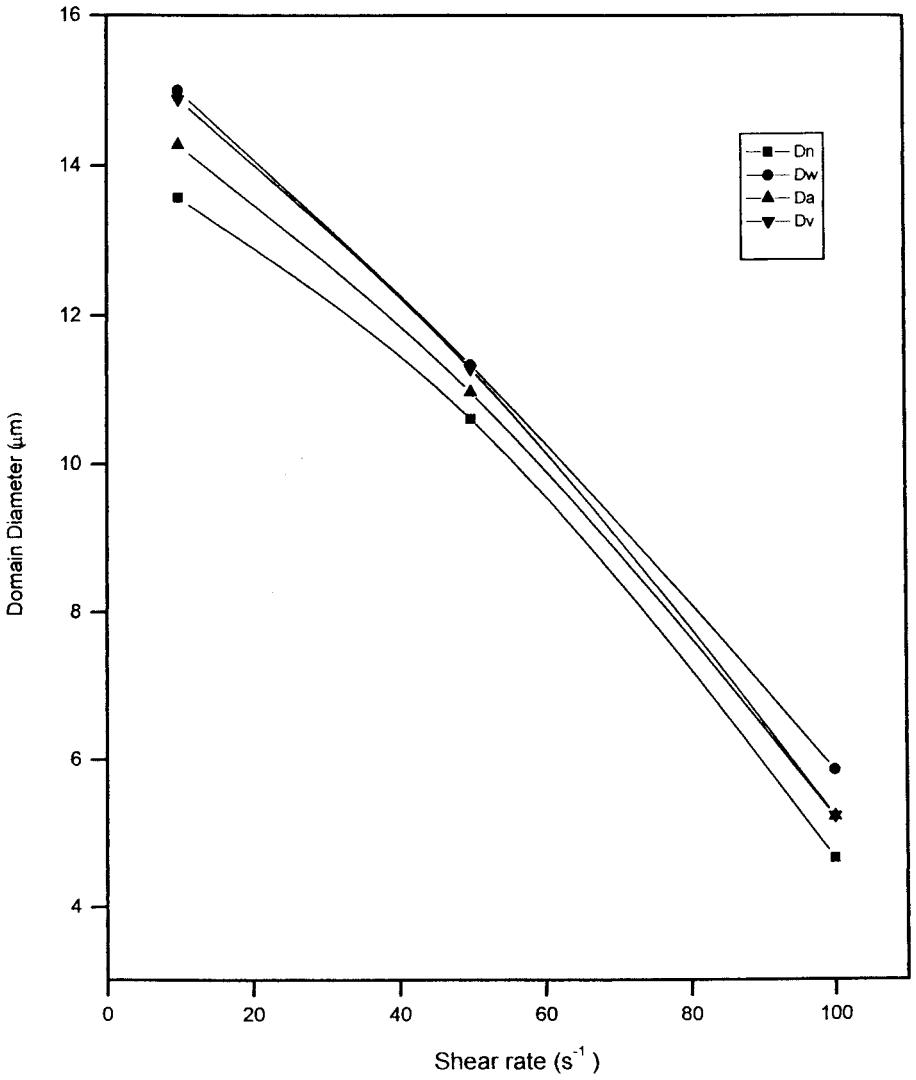

Figure 13 Effect of shear rate on particle size.

$$\ln \eta_{mix} = \frac{\phi_1(\alpha - 1 - \gamma\phi_2)\ln \eta_1 + \alpha\phi_2(\alpha - 1 + \gamma\phi_2)\ln \eta_2}{\phi_1(\alpha - 1 - \gamma\phi_2) + \alpha\phi_2(\alpha - 1 + \gamma\phi_1)} \quad \text{Model 4} \tag{18}$$

where

$$\alpha = f_2/f_1 \tag{19}$$

and

$$\gamma = \beta/f_1 \tag{20}$$

f_1 and f_2 are free-volume fractions of components 1 and 2, respectively, and β is an interaction parameter:

$$f = f_g + \alpha(T - T_g) \tag{21}$$

where $fg = 0.025$:

$$\alpha_{fm} = B/2.303C_1C_2 \tag{22}$$

where $B = 0.9 \pm 0.3 \approx 1$, $C_1 = 17.44$, and $C_2 = 51.6$ K. For the calculations, the value of γ was varied to obtain best-fit values with the experimental results.

In Figure 11, the viscosity values obtained from the theoretical models and from the experiment for different blend compositions at a shear rate of 50 s^{-1} are plotted. It is evident from Figure 11 that the viscosities of the blends show a negative deviation from the additivity rule and the experimental curve lies between Hashin's upper- and lower-limit models.

From this theoretical modeling, the melt viscosity calculated for the different blend compositions shows a negative deviation from the additivity rule, indicating the immiscibility of the blends. This is associated with the heterogeneous nature of the components as well as the high interlayer slip between the phases.

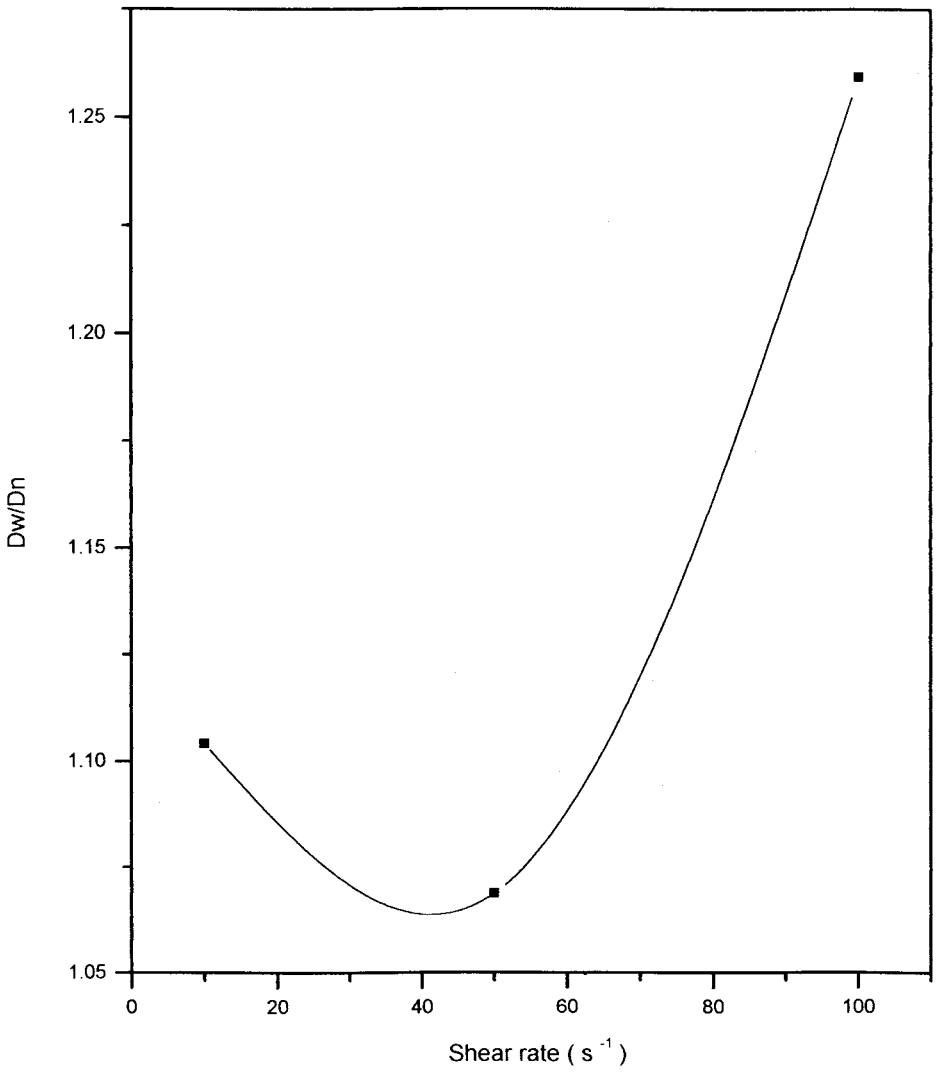

Figure 14 Effect of viscosity ratio on particle size.

In the case of the model suggested by Sood et al.,[39] the viscosity values can be better explained with $\gamma = -0.19$. This value of γ corresponds to an interaction parameter, $\beta = -1.666 \times 10^{-2}$ according to the equation $\beta = \gamma f_1$.

Extrudate morphology

The cryogenically broken extrudates were subjected to a solvent-etching process to remove one phase from the blend. The samples dried in an air oven were examined under an SEM. The SEMs of PS/nylon 6 (70/30) at 230°C for shear rates at 10, 50, and 100 s^{-1} are given in Figure 12(a–c), respectively. From the SEMs, it is evident that there is a decrease in the particle size with an increase in the shear rates. The dependence of the domain diameter and the shear rate is plotted in Figure 13. At a higher shear rate, the dispersed particles in the blend are elongated at the entrance of the capillary. This structure is unstable and breaks up into smaller droplets, resulting in a reduced domain size. At the entrance of the capillary, the particles will be elongated and then will undergo a severe breakdown depending on the shear rate. Again, at high shear rates, the extent of the breakup will be higher.

As suggested earlier, the decrease in the viscosity of the system with the shear rates can also be attributed to the decrease in the particle size. The decrease in the particle size is due to the increased deformation and the consequent breakdown of the particles with an increased shear rate. The effect of the viscosity ratio on the average domain diameter was studied. The results are plotted in Figure 14. It is evident from the figure that the particle size approaches the minimum when the viscosity ratio approaches unity.

Figure 15 compares the Taylor limit and the prediction from Wu's correlation, at varying shear rates to the experimental observation. The Taylor limit, however, does not account for the non-Newtonian effects

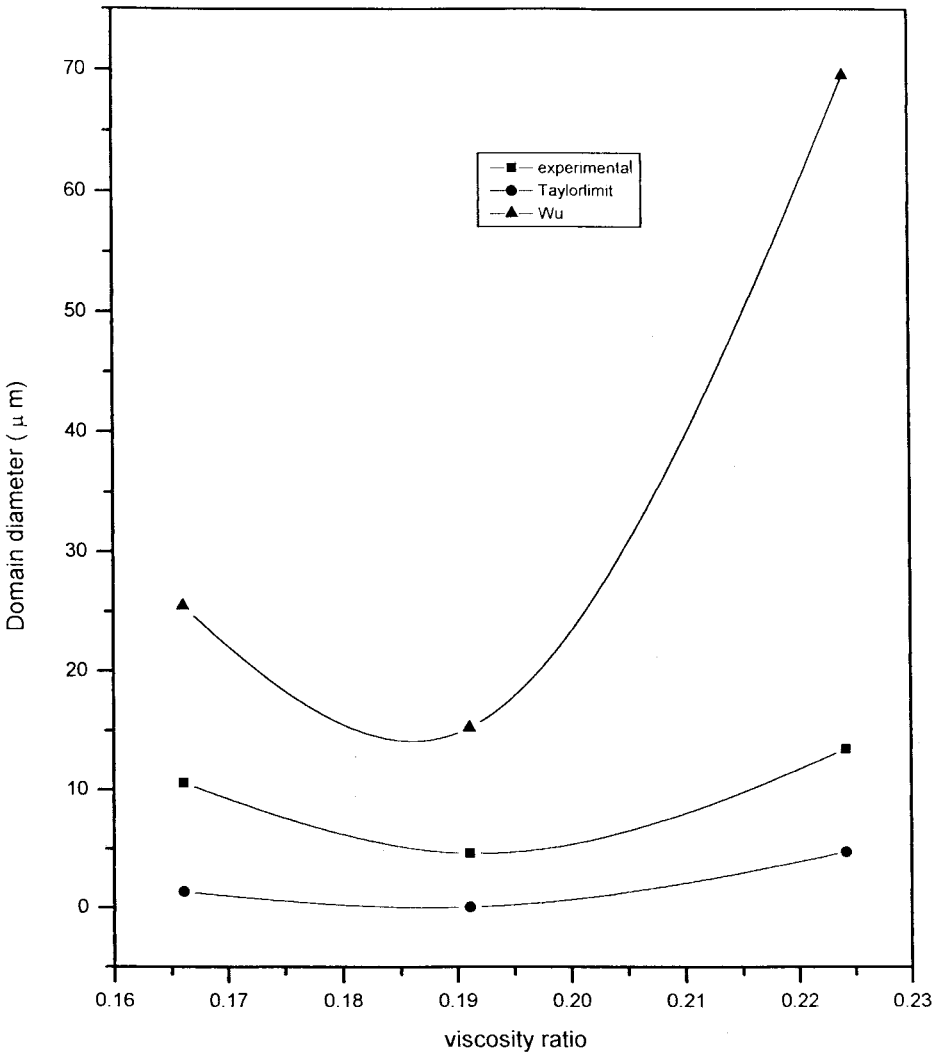

Figure 15 Comparison of Taylor and Wu's prediction.

present in the system. Polymer mixers have extensional flows in addition to simple shear flow, but extensional flows produce even finer dispersions than do simple shear flows. The experimental values lie in between the two models.

CONCLUSIONS

The phase morphology development in nylon/PS blends as a function of the blend composition, mixing time, and rotation speed was investigated. The morphology indicated a two-phase structure, and in all cases, the minor component forms the dispersed phase and the major component forms the continuous phase. The 50/50 nylon/PS composition exhibited a cocontinuous morphology. The size of the dispersed phase was found to increase with its concentration. This phenomenon can be attributed to the coalescence of the particles and the fibrillation of nylon. The effect of the mixing time showed that the most significant breakdown occurred during the initial 3 min of mixing. The domain size was most affected when the rotor speed was increased from 9 to 20 rpm, followed by a leveling-off at higher rotor speeds. The continuity of the blends was calculated by the solvent-extraction technique, which again confirmed that both phases are almost continuous at a 50/50 blend composition. The melt viscosity of the system decreased with increase in the shear rate, indicating pseudoplastic behavior. As the PS content increased, the melt viscosity of the system decreased. The negative deviation of the measured viscosity from the additivity rule indicates the immiscibility of the blends resulting from the heterogeneous nature of the components and due to the high interlayer slip between the phases. The extrudate morphology indicated that the particle size diminishes considerably at higher shear rates. The 50/50 PS/nylon blend showed cocontinuous morphology, while the other blend compositions showed a dispersed-phase morphology. The influence of the viscosity ratio

on the particle size indicates that the particle size is the lowest when the viscosity ratio approaches unity. The experimentally obtained domain diameters at various shear rates were compared with the Taylor limit and the prediction from Wu's correlation. The experimental value lies between the two models.

The authors are thankful to DSM (Netherlands) and Polychem (Mumbai, India) for providing the materials.

References

1. Polymer Blends and Alloys; Folkes, M. J.; Hope, D. S., Eds.; London: Blackie, 1993.
2. Dao, K. C. Polymer 1984, 25, 1527.
3. Gergen,W. P.; Lutz, R.; Davison, S. In Thermoplastic Elastomers: A Comprehensive Review; Legge, N. R.; Holden, G.; Davison, S., Eds.; Munich, Germany: Carl Hanser, 1987; p 507.
4. Polymer Blends; Paul, D. R.; Newman, S.; Eds.; Academic: New York, 1978; Vol. 1, Chapter 1, p 11.
5. Gattiglia, E.; La Mantia, F. P.; Turturro, A.; Valenza, A. Polym Bull 1989, 21, 47.
6. Chov, G. D.; Kim, S. H.; Jo, W. H. Polym J 1996, 6, 52.
7. Brydson, J. A. Flow Properties of Polymer Melts, 2nd ed.; George Godwin: London, 1981.
8. Van Oene, H. Colloid J Interface Sci 1972, 40, 448.
9. Uttracki, L.; Sammut, P. Polym Eng Sci 1990, 17, 1027.
10. Acierno, D.; Demma, G. Eur Polym J 1990, 26, 1049.
11. Varghese, H.; Bhagawan, S. S.; Thomas, S. Polym Plast Technol Eng 1999, 38, 319.
12. Asaletha, R.; Kumaran, M. G.; Thomas, S. J Appl Polym Sci 1998, 69, 2673.
13. George, J.; Ramamurthy, K.; Varughese, K. T.; Thomas, S. J Polym Sci Part B Polym Phys 2000, 38, 1104.
14. eorge, S.; Ramamurthy, K.; Anand, S.; Groeninckx, G.; Varughese, K. T.; Thomas, S. Polymer 1999, 40, 4325.
15. Gorton, D. T.; Pendle, T. D. NR Technol 1981, 12, 1.
16. Danesi, S.; Porter, R. S. Polymer 1978, 19, 448.
17. Tsebrenko, M .V.; Rezenova, N. M.; Vingradov, G. V. Polym Eng Sci 1980, 20, 1023.
18. Straita, J. M. Trans Soc Rheol 1972, 16, 339.
19. Heikens, D. N.; Hoen, W.; Barensten, P.; Piet, H.; Laden, J Polym Sci Polym Symp 1978, 62, 309.
20. Dao, K. C. Polymer 1994, 25, 15278.
21. Heikens, D.; Barensten, W. M. Polymer 1977, 18, 69.
22. Thomas, S.; Groeninckx, G. J Appl Polym Sci 1999, 61, 2383.
23. Thomas, S.; Prud'homme, R. E. Polymer 1992, 33, 4260.
24. Bourry; Favis, J Polym Sci Part B Polym Phys 1998, 36, 1889.
25. Jordhamo, G. M.; Manson, J. A.; Sperling, L. H. Polym Eng Sci 1986, 26, 517.
26. Chen, T. H.; Su, A. C. Polymer 1993, 34, 4826.
27. Everaet, V.; Aerts, L.; Groeninckx, G. Polymer 1999, 43, 6627.
28. Min, K.; White, J. L.; Fellers, J. F. J Appl Polym Sci 1984, 29, 2117.
29. Elmendrop, J. J.; vander Vegt, A. K. Polym Eng Sci 1986, 26, 1332.
30. Roland, C. M.; Bohm, G. G. A. J Polym Sci Polym Phys 1984, 22, 79.
31. Taylor, G. I. Proc R Soc Lond A 1932, 138, 41.
32. Taylor, G. I. Proc R Soc Lond A 1934, 146, 501.
33. Favis, B. D. J Appl Polym Sci 1990, 39, 285.
34. Sundararaj, U.; Macosko, C. W.; Rolando, R. J.; Chan, H. T. Polym Eng Sci 1992, 32, 1814.
35. Wu, S. Polym Eng Sci 1987, 27, 35.
36. Chen, J.; Hahn, P. S.; Slattery, J. C. AIChE J 1984, 30, 662.
37. Schreiber, H. P.; Olguin, A. Polym Eng Sci 1983, 23, 129.
38. Uttracki, L. A.; Sammut, P. Polym Eng Sci 1988, 28, 1405.
39. Sood, K.; Dutta, R.; Mashelkar, A. Polym Eng Sci 1988, 68, 67.